

# SANDIA REPORT

SAND2019-10685

Printed Click to enter a date



Sandia  
National  
Laboratories

# Characterization of Distributed Phase Plates for use on Z-Beamlet

Matthias Geissel, Jens Schwarz, Ian C. Smith, Jonathon E. Shores

Prepared by  
Sandia National Laboratories  
Albuquerque, New Mexico  
87185 and Livermore,  
California 94550

Issued by Sandia National Laboratories, operated for the United States Department of Energy by National Technology & Engineering Solutions of Sandia, LLC.

**NOTICE:** This report was prepared as an account of work sponsored by an agency of the United States Government. Neither the United States Government, nor any agency thereof, nor any of their employees, nor any of their contractors, subcontractors, or their employees, make any warranty, express or implied, or assume any legal liability or responsibility for the accuracy, completeness, or usefulness of any information, apparatus, product, or process disclosed, or represent that its use would not infringe privately owned rights. Reference herein to any specific commercial product, process, or service by trade name, trademark, manufacturer, or otherwise, does not necessarily constitute or imply its endorsement, recommendation, or favoring by the United States Government, any agency thereof, or any of their contractors or subcontractors. The views and opinions expressed herein do not necessarily state or reflect those of the United States Government, any agency thereof, or any of their contractors.

Printed in the United States of America. This report has been reproduced directly from the best available copy.

Available to DOE and DOE contractors from

U.S. Department of Energy  
Office of Scientific and Technical Information  
P.O. Box 62  
Oak Ridge, TN 37831

Telephone: (865) 576-8401  
Facsimile: (865) 576-5728  
E-Mail: [reports@osti.gov](mailto:reports@osti.gov)  
Online ordering: <http://www.osti.gov/scitech>

Available to the public from

U.S. Department of Commerce  
National Technical Information Service  
5301 Shawnee Rd  
Alexandria, VA 22312

Telephone: (800) 553-6847  
Facsimile: (703) 605-6900  
E-Mail: [orders@ntis.gov](mailto:orders@ntis.gov)  
Online order: <https://classic.ntis.gov/help/order-methods/>



## ABSTRACT

Distributed Phase Plates (DPP) are used in laser experiments to create homogenous intensity distributions of a distinct shape at the location of the laser focus. Such focal shaping helps with controlling the intensity that is impeding on the target. To efficiently use a DPP, the exact size and shape of the focal distribution is of critical importance.

We recorded direct images of the focal distribution with ideal continuous-wave (CW) alignment lasers and with laser pulses delivered by the Z-Beamlet facility. As necessary to protect the imaging sensors, laser pulses will not be performed by full system shots, but rather with limited energy on so-called ‘rod-shots’, in which Z-Beamlet’s main amplifiers do not engage. The images are subsequently analyzed for characteristic radii and shape. All characterizations were performed at the Pecos target area of Sandia with a lens of 3.2 m focal length.

## CONTENTS

1. Scope .....	8
1.1. Background and Legacy .....	9
1.2. Requirements .....	10
2. Setup .....	11
3. Focus Measurements .....	12
3.1. Characteristics of the SNL1300 Phase Plate .....	13
3.2. Characteristics of the LLE2000 Phase Plate .....	17
3.3. Characteristics of the LLE800 Phase Plate .....	18
3.3.1. Angular intensity variations .....	18
3.4. Characteristics of the SNL750 Phase Plate .....	19
3.5. Characteristics of the SNL1100 Phase Plate .....	21
3.5.1. Focus shape with phase plate reversal .....	22
3.6. Characteristics of the SNL1500 Phase Plate .....	23

## LIST OF FIGURES

Figure 1-1. Conceptual sketch of the influence of a DPP. Specific areas of the DPP induce slight angles to sections of the laser beam, causing it to be focused at a different position. Each focus position is addressed multiple times. A good DPP can cover a closed area of arbitrary shape very evenly (unlike this cartoon) through continuous slope variations. The image on the right shows details of an actual spot measurement with the LLE1900 DPP. Circles highlight diffraction limited speckles (resolution: 4.4 $\mu\text{m}/\text{px}$ ) .....	9
Figure 2-1. Cartoon of the measurement setup for the laser focus analysis with a DPP .....	11
Figure 3-1. Examples for measurements with the SNL1300 phase plate in focus and 10 mm out of focus. Even at full resolution the modulation of the spot is not very high since the required exposure time lead to some motion blur, which was caused by pointing fluctuations of the laser .....	13
Figure 3-10. Characterization of the SNL750 phase plate .....	21
Figure 3-11. SNL1100 beam waist. Actual data points are not shown. Plots represent a Gaussian approximation of the measured data points .....	22
Figure 3-12. Comparison of encircled energies for forward and reverse phase plate insertions. The abbreviation ‘CPP’ stands for ‘continuous phase plate’ and is synonymous to ‘distributed phase plate (DPP)’, depending on the terminology of individual laser facilities .....	22
Figure 3-13. Characterization of the SNL750 phase plate .....	23
Figure 3-14. Specific diameter/energy combinations (left) and beam waist data (right) for the SNL1500 phase plate. The waist is practically flat over an depth exceeding $\pm 1$ mm .....	24

## LIST OF TABLES

Table 2-1. Comparison of available laser sources for DPP measurements .....	11
Table 3-1. Comparison of all phase plates used and characterized by Z-Beamlet .....	12
Table 3-1. List of Encircled energy diameters for the SNL1500 phase plate (all diameter measurements in mm) .....	24

This page left blank

## ACRONYMS AND DEFINITIONS

Abbreviation	Definition
$1\omega$	“One-Omega”, the fundamental wavelength of the Z-Beamlet laser at 1053 nm.
$2\omega$	“Two-Omega”, the second harmonic wavelength of Z-Beamlet at 527 nm.
CPP	Continuous Phase Plate (same as ‘distributed phase plate’)
CW	Continuous Wave (laser)
D $n\%$	Diameter that encircles $n\%$ of the total laser energy. E.g.: D95 encircles 95% of the energy.
DPP	Distributed Phase Plate (same as ‘continuous phase plate’)
Frame	Single still image acquired by X-ray backlighting with Z-Beamlet. Two Frames can be recorded with the Multi-Frame-Backlighter option (see “ <b>MFB</b> ”). Synonymously used for the alignment lasers and beam paths that are used to produce these images.
Full System Shot	A laser shot in which all amplifiers are activated, as compared to a low energy “ <b>Rod-Shot</b> ”. Z-Beamlet’s full system shots can deliver several kilojoules in a few nanoseconds.
FWHM	Diameter at which the intensity reaches half of the peak average intensity as defined with Fig. 0-1.
High-Bay, HiBay	Room 101 in SNL’s Building 986, which houses the Z-Beamlet and Z-Petawatt lasers. The lasers can be transported to dedicated target chambers (see “ <b>Target Bay</b> ”) or into <b>Z</b> .
Jemez	The Jemez target chamber in SNL’s Building 983, Room 1303 (“Target Bay”), which uses a 2 m focal length to focus Z-Beamlet onto a target
LEH	Laser-Entrance-Hole: Aperture through which a laser enters to hit a target (or heat a gas filled volume). Sometimes also used to refer to the window that covers the Laser-Entrance-Hole.
LLE	The Laboratory for Laser Energetics at the University of Rochester.
MagLIF	Magnetized Liner Inertial Fusion
Main Amplifiers	Last amplification stage of a laser system. Z-Beamlet uses 11 amplifiers which can accommodate a square beam size of roughly 31 cm x 31 cm. The laser media in these amplifiers are Nd:glass slabs. The main amplifiers can affect the beam quality through thermal stress distortions, which are induced by firing the pump flash lamps.
MFB	Multi-Frame Backlighting: A capability for the Z-Beamlet laser that enables the acquisition of two X-ray images (“Frames”) at two different times, several nanoseconds apart, and/or two different photon energies. Z-Beamlet accomplishes this with splitting the output in two pulses with slightly different angle and collimation, thus enabling to hit two different targets at different times. The laser focus for each frame is marked with a dedicated alignment laser.
ND	Neutral Density: Neutral Density filters attenuate light without discrimination of the wavelength. The values are following a logarithmic scale on base 10 (i.e.

Abbreviation	Definition
	ND1=10x, ND2=100x).
Pecos	The Pecos target chamber in SNL's Building 983, Room 1303 ("Target Bay"), which uses a 3.2 m focal length to focus Z-Beamlet onto a target. Main target chamber used for this report.
Quasi Full System Shot	A shot with all amplifiers activated, but the <b>Main Amplifiers</b> are mistimed by 1 ms (early). This represents a " <b>Rod-Shot</b> " with all the thermal distortions that are induced by the main amplifiers' pump flash lamps and it is meant to simulate the spot profile of a full system shot.
Rod, Rod-Shot	Last stage of pre-amplification for large laser systems. The laser medium is an Nd:Glass rod. Energies for Z-Beamlet can reach just over one joule at this stage, which is sufficient to create enough green light in the KTP conversion crystal to be comparable to the brightness of the alignment lasers in the <b>Target Bay</b> .
SNL	Sandia National Laboratories
Target Bay	Room 1303 in SNL's Building 983, housing a variety of target chambers for 'laser-only' experiments (see <b>Jemez, Pecos</b> ).
Z	Axis of the laser propagation or laser beam direction. Z=0 marks the position of the best focus.
<b>Z</b> , Z-Machine	Sandia's Z-Accelerator.
ZBL	The Z-Beamlet laser.

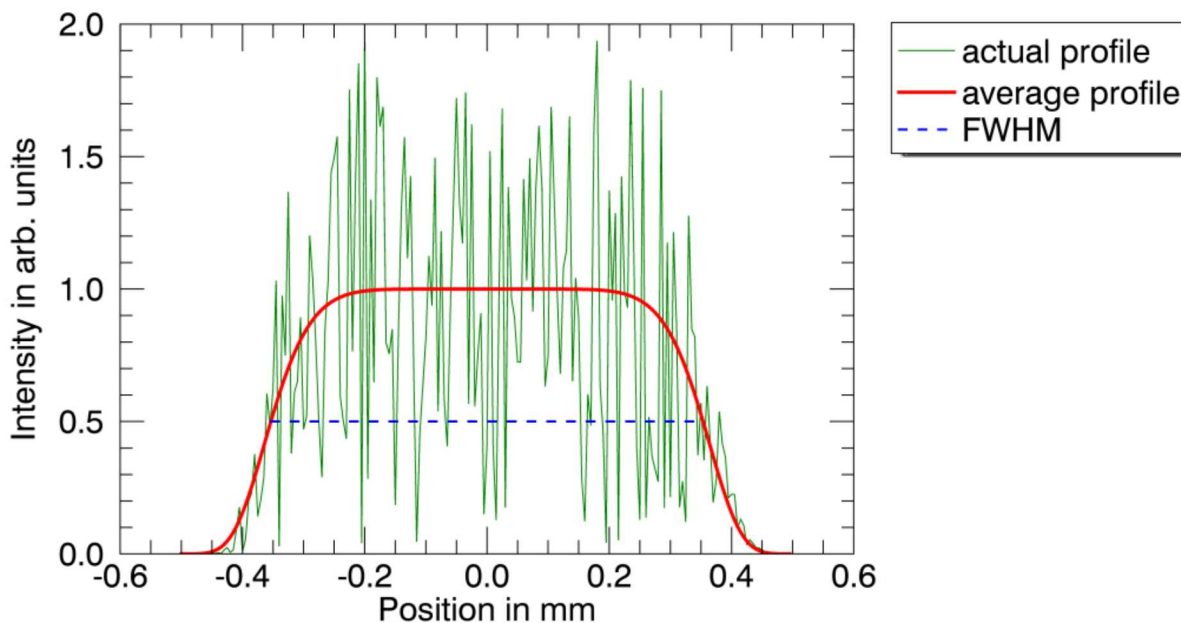


Fig. 0-1: Definition of the FWHM for DPP-shaped laser spots.

## 1. SCOPE

This memo is intended to document several measurement campaigns that characterized the performance of distributed phase plates (DPPs) for Z-Beamlet. ORG-01682 owns four phase plate types, which produce smooth circular focal spots with diameters from just below 1 mm to over 2 mm. The exact diameter depends on the specifics of the incident laser beam.

Much of the motivation to use phase plates at Sandia comes from the desire to have the best possible control over the laser intensity on target in conjunction with a minimization of localized high intensity clusters in the profile, which can lead to enhanced laser plasma instabilities and resulting negative effects, such as reduced energy coupling to the target and intensity deflection towards surfaces that shall stay pristine. Phase plates are still subject to interference speckles, resulting from the coherent nature of laser light, which also modulate the intensity distribution strongly, but the microscopic size of the speckles causes a rapid smoothing of any temperature gradients in the plasma at focus, which strongly reduces the above mentioned negative effects of intensity modulation.

## 1.1. Background and Legacy

A variety of experiments may require illuminating an extended area with high intensity lasers rather than hitting a target with the best focus. Such experiments can be driving planar shocks or heating a gas without generating too strong laser-plasma-instabilities. The latter can also require to use a low enough intensity to be fully absorbed at a given gas density and volume. In both cases it is imperative to have a well-known intensity distribution of the laser, since irregularities can cause instabilities in the hydrodynamics and significantly complicate modeling the experiment. While Gaussian beams (beams with a Gaussian cross-section) always keep the same beam profile independent on their size when being focused, non-Gaussian beams have different profiles in the collimated beam ('near field') and in the focus ('far field'). This is particularly important for beams with sharp gradients, such as a 'flat-top' beam that follows a high-order Supergaussian cross section. Flat-top profiles dominate the world of high energy lasers, since they deplete the amplifier medium more efficiently. Illuminating an area with a defocused flat-top laser beam is an option if the area is large enough to keep the laser beam in the 'near-field' regime, which is essentially just a demagnified laser beam profile. Once the profile gets small enough to be near the best focus within less than a percent of the focal length, the profile changes and assumes a shape that is rarely predictable, crossing a regime known as intermediate field. Laser profiles in the intermediate field typically exhibit large intensity variations across the beam, often with pronounced hot spots and asymmetries. To create a smooth distribution covering the area of a typical intermediate field spot, one can employ DPPs as sketched in Fig. 1 (left). A DPP uses slight slope variations across the optic, which redirect portions of the beam to different areas focus positions. A perfect incoming phase-front would be modified such that a predetermined area is illuminated. In addition, every illuminated part of the focus contains laser light originating from multiple parts of the optic, which effectively randomizes the contributions of phase-front errors in an imperfect laser beam. As a result, one achieves a very even beam profile, which is modulated with interference speckles on small spatial scales (diffraction limit of the focusing optic, see Fig. 1-1, right).

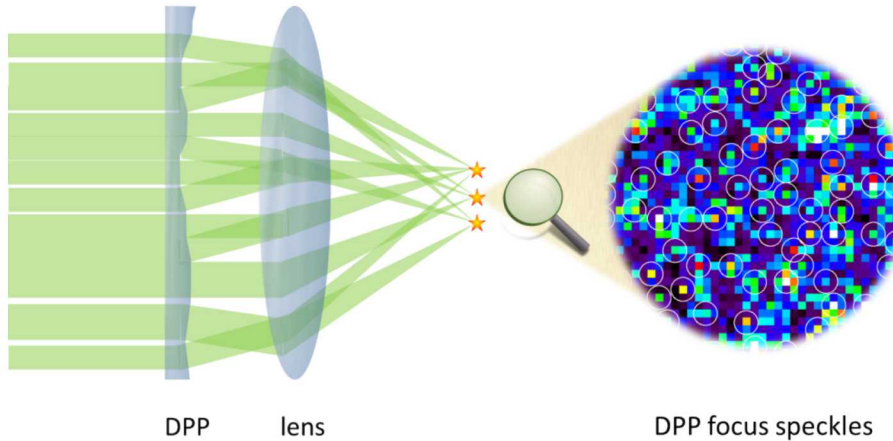


**Figure 1-1.** Conceptual sketch of the influence of a DPP. Specific areas of the DPP induce slight angles to sections of the laser beam, causing it to be focused at a different position. Each focus position is addressed multiple times. A good DPP can cover a closed area of arbitrary shape very evenly (unlike this cartoon) through continuous slope variations. The image on the right shows details of an actual spot measurement with the LLE1900 DPP. Circles highlight diffraction limited speckles (resolution: 4.4  $\mu\text{m}/\text{px}$ ).

## 1.2. Requirements

A satisfying characterization should include radii of illumination for varying definitions of spot size, since the DPP creates a spot with ‘soft’ edges. Hence the definition of the spot may depend on the application. If used with different incident laser beams (e.g. CW alignment beam and pulse amplified beam), the performance for both cases may be important. It is also of interest for heating experiments to characterize the size of the spot with respect to focal depth. We will call this a beam-waist measurement.

## 2. SETUP

While spot profiles were traditionally looked at with microscope optics, recent improvements in CCD and CMOS camera technology enable us to image a laser directly on the sensor and resolve small structure variations of the laser spot at or near the diffraction limit. This has the advantage that alignment artifacts such as coma or astigmatism are eliminated. The only remaining optical element necessary for focal imaging are neutral density filters, which attenuate the laser intensity to accommodate the dynamic range of the camera. By placing the camera and ND-filters on a linear translation stage, we can find best focus and measure the evolution of the focus spot with respect to focal depth. Figure 3 shows the setup used in the Pecos target chamber for the measurements used in this report (not to scale).

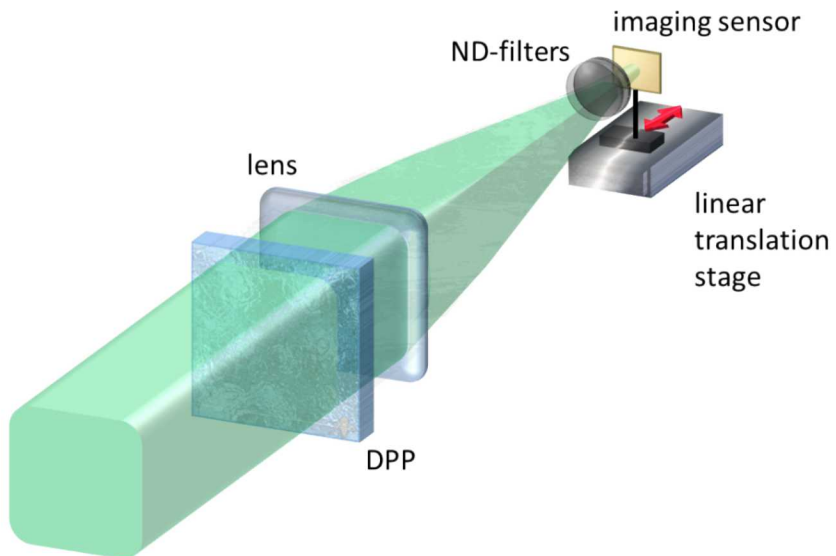


**Figure 2-1. Cartoon of the measurement setup for the laser focus analysis with a DPP.**

Three different measurements are possible to assess the performance of the DPP, using three different types of laser. They can point to either position of the “Multi-Frame Backlighter” (MFB) positions which are available for Z-Beamlet. Heating experiments for Magnetized Liner Inertial Fusion (MagLIF) use the “Frame 1” position. The minimum focus size has an influence on the resulting spot size and edge-definition with a DPP. Table 2-1 compares the different laser sources.

**Table 2-1. Comparison of available laser sources for DPP measurements.**

Laser	Wave Type	Best Focus Size	Source Propagation	Rep. Rate	MFB Position
Alignment 1	Continuous	200 $\mu\text{m}$	Fiber	N/A	Frame 1
Alignment 2	Quasi-CW	20 $\mu\text{m}$	Free-air	20 kHz	Frame 2
Rod Shot	pulsed	200 $\mu\text{m}$	Free-air	5 min.	Frame 1 or 2
Quasi Full System Shot	pulsed	200 $\mu\text{m}$	Free air	3 hrs.	Frame 1 or 2

### 3. FOCUS MEASUREMENTS

Six different DPPs have been used with Z-Beamlet, partly being on loan from the Laboratory for Laser energetics (LLE), and partly being owned by Sandia. Most designs have been developed by LLE for the Omega-EP laser. Table 3-1 shows an overview of the DPPs being used and defines their nomenclature.

**Table 3-1. Comparison of all phase plates used and characterized by Z-Beamlet**

DPP	Owned by	Designed for	Design wavelength	Design focal length	Design spot diameter	Z-Beamlet spot diameter <sup>+</sup>
SNL1300	Sandia	Z-Beamlet	527nm	2 m	1.3 mm FWHM 1.62 mm D95*	2.08 mm FWHM 2.60 mm D95
LLE2000	LLE	Omega-EP	351nm	3.4 m	1.87 mm D95*	1.76 mm D95
LLE800	LLE	Omega-EP	351nm	3.4 m	800 $\mu$ m D95	753 $\mu$ m D95
SNL750	Sandia	Omega-EP	351nm	3.4 m	736 $\mu$ m D95*	693 $\mu$ m D95
SNL1100	Sandia	Omega-EP	351nm	3.4 m	1060 $\mu$ m D95*	998 $\mu$ m D95
SNL1500	Sandia	Z-Beamlet	527nm	3.2 m	1.5 mm D95	1.5 mm D95

\*:  $\pm 15 \mu$ m in radius acc. to drawing; <sup>+</sup>: Calculation for 3.2 m focal length ignoring wavelength differences.

Table 3-1 also shows the expected spot size for use with an  $f=3.2$  m lens. This calculation ignores the influence of changing wavelengths. Since the DPP is creating a certain spot size purely by redirecting portions of the beam, the wavelength only enters through changes in the material's index of refraction. This is a small effect compared to the changes in focal length or wavefront distortions.

The following sections describe the characterizations of phase plates in a chronological order (as used and/or purchased by Sandia).

### 3.1. Characteristics of the SNL1300 Phase Plate

The SNL1300 phase plate was originally acquired to be used in material stress experiments in collaboration with the University of Texas at Austin. At the time, so-called “ZBL Cal-Chamber”, was equipped with a lens of 2 m focal length, which is now used in the Jemez target chamber.

The design goal for the phase plate was originally 2 mm, but the required mechanical structures in the optic were not achievable by the manufacturer at the time, and the design was updated during production to the largest safely producible spot size: 1.3 mm (FWHM). The unusual process likely limited the overall quality of the spot shape. The actual SNL1300 was used for Laser-Entrance-Hole (LEH) window transmission measurements in the context of MagLIF. SNL1300 has never been used in [Z](#).

Measurements with the “Frame 1” alignment beam for the characterization of SNL1300 in Pecos were performed in September 2014. Fig. 3-1 shows data taken at best focus and for the profile that was taken 10 mm behind best focus.

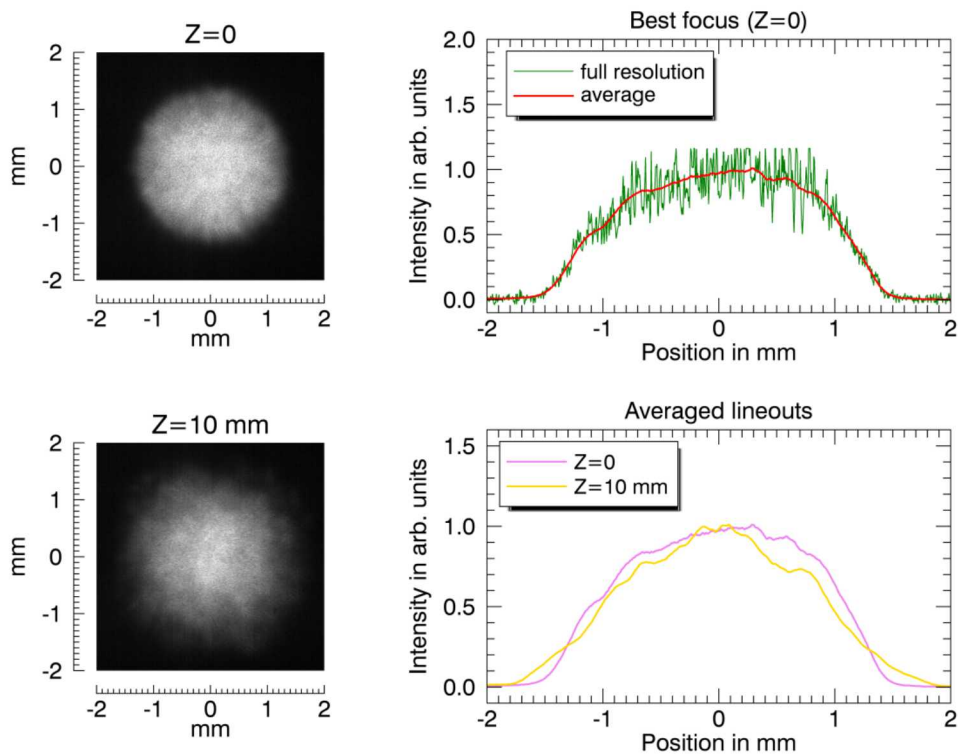


**Figure 3-1. Examples for measurements with the SNL1300 phase plate in focus and 10 mm out of focus. Even at full resolution the modulation of the spot is not very high since the required exposure time lead to some motion blur, which was caused by pointing fluctuations of the laser.**

Profiles have been recorded at various positions around best focus, and Fig. 3-2 shows a more comprehensive evaluation of the data. It is noteworthy that D95 grows when defocusing - as one would expect -, while the FWHM decreases with defocus, since the softening of the edges dominates over the growth of the total spot size. This behavior is typical for all phase plates and will not be investigated for the other DPPs.

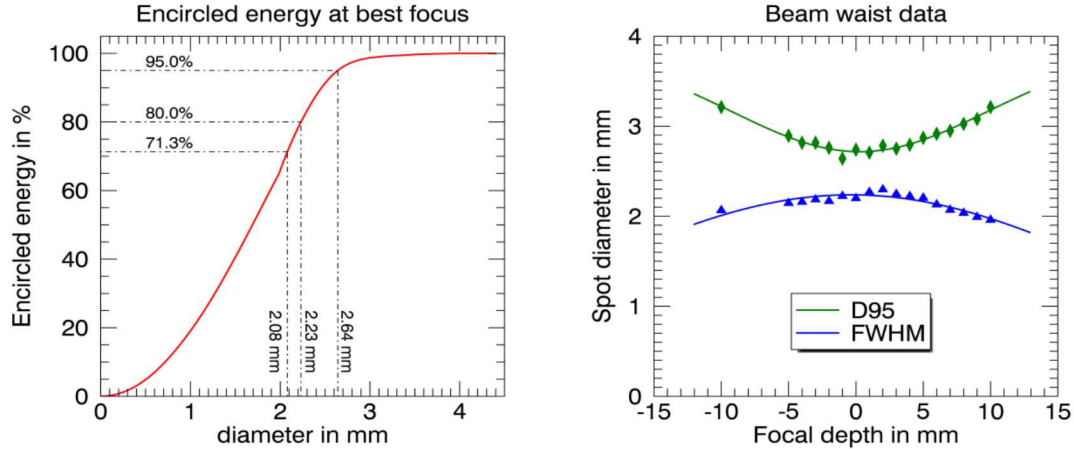


**Figure 3-2. : Analysis of the most important data for the SNL1300 phase plate. It contains only 71.3% of the energy at the predicted FWHM. The actual FWHM contains 80% of the energy. The industry standard D95 measures to 2.64 mm at best focus. The beam waist measurements are indicated with symbols, while the solid lines represent a Gaussian approximation to the data. The spot stays essentially the same within 2 mm around the best focus.**

Since the alignment beam is just a convenient surrogate for the amplified pulse of Z-Beamlet, measurements at best focus were done with rod-shots and an intentionally mistimed full-system shot. For the latter we fired the main amplifiers of Z-Beamlet about one millisecond too early, which is early enough to prevent amplification of the rod-shot level energies, but close enough to the laser pulse to maintain the flash lamp induced distortions that are created by thermal stress on regular full system shots. Figure 3-3 shows a summary of the analyzed data for these pulsed measurements.

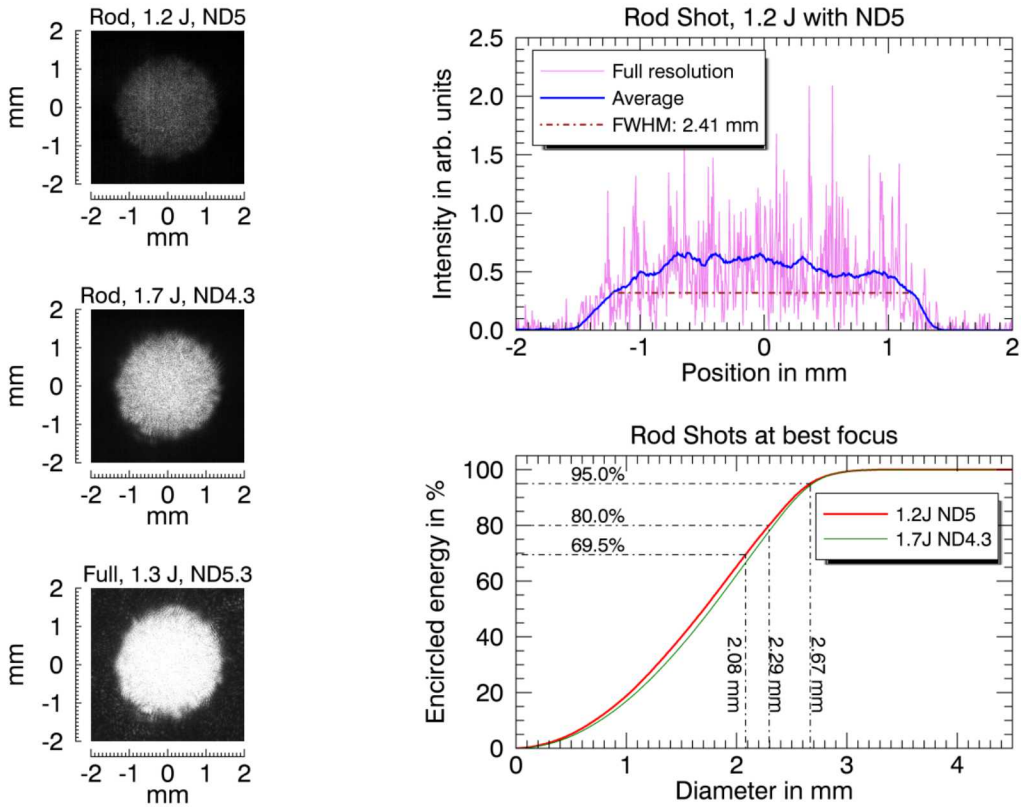


**Figure 3-3. Summary of rod-shot analyses for the SNL1300 phase plate. Since the exposure is reduced to a laser pulse length of one nanosecond, there is no more motion blur and the spot profile exhibits a very deep modulation. A quasi full system shot was strongly overexposed and not suited for a more detailed analysis. It must have gained some unaccounted amplification beyond 1.3 J by the decaying inversion of the main amps.**

While the FWHM seems to have grown slightly for the rod shot, the D80 and D95 values, and the encircled percentage at D=2.08 mm are within 3% of the Frame1-CW data. A slightly overexposed rod-shot (1.7J/ND4.3) yields a slightly larger spot, since energy in the center is virtually lost due to over-exposure and the statistical weight of the outer regions of the spot increases. But at this moderate overexposure the increase is negligible. However, the quasi full system shot is more strongly overexposed and appears visibly larger. The lower intensity edges get artificially boosted to the level of the top intensity, thus broadening the spot. In light of this effect, it is reasonable to assume that a balanced exposure would have given very similar results to the rod shot.

To estimate the spot size on a fully amplified shot, an experiment using the SNL1300 phase plate with a titanium target was performed. Figure 7 shows the vertical and horizontal lineouts through the titanium K-shell emission, which should represent a softened image of the laser spot. The emission can be approximated very well assuming a 3rd order super-Gaussian profile with a variance  $\sigma$  of 0.69 mm, where the super-Gaussian function of order n is defined as by Eq. 1.

$$F(x) = \text{EXP} \left( -\sqrt{\left( \frac{x - x_0}{\sigma} \right)^{2n}} \right) \quad (1)$$

This leads to approximately the same footprint as measured on the camera for the unamplified beam. The FWHM for this function is 1.54 mm. The softer edges are likely due to the time-integrated nature of the image, assuming that the edges cool faster than the center, thus producing a ‘narrower top’ of the intensity distribution.

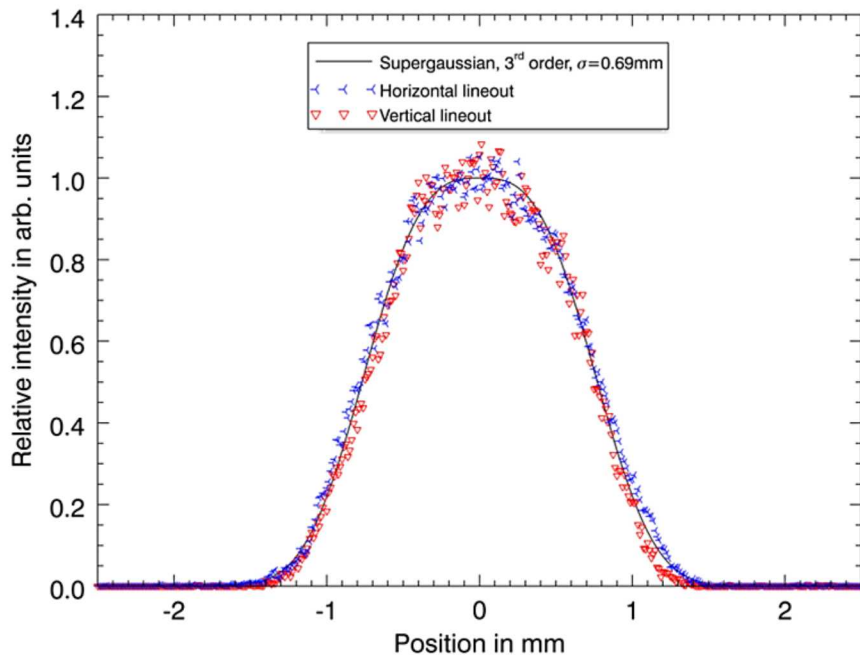


**Figure 3-4. Lineouts for the K-shell emission of a Ti-target that was hit by Z-Beamlet with the SNL1300 phase plate.**

### 3.2. Characteristics of the LLE2000 Phase Plate

First MagLIF experiments with a DPP were carried out in the beginning of 2015 using a D95=1.87 mm phase plate from LLE in Rochester. Since the DPP is designed for 3.4 m focal length, one would expect a 1.76 mm spot size for 3.2 m focal length with Z-Beamlet. Measurements were done with a CW alignment beam and a number of rod-shots.

Measurements with the alignment beam resulted in a D95 diameter of 1.8 mm as shown in the focal envelope plot of Fig. 3-5a, while a measurement with a pulsed rod-shot resulted in a D95 value of 1.72 mm (encircled energy plot; Fig. 3-5b).

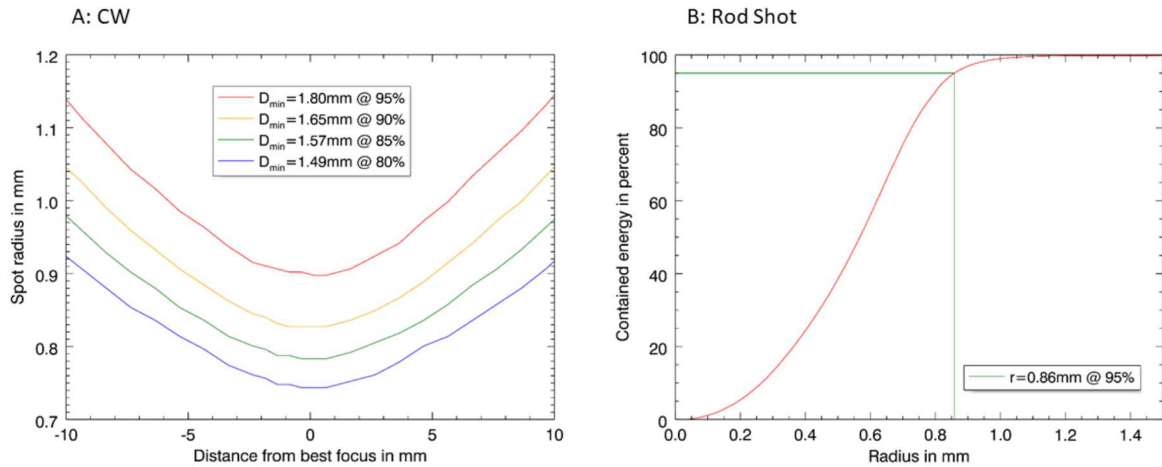


**Figure 3-5. Measured profile plots for the LLE2000 phase plate.**

The LLE2000 phase plate was not used for very long at Sandia and therefore was not characterized in as much detail as other variants.

### 3.3. Characteristics of the LLE800 Phase Plate

The LLE800 phase plate was characterized with both available CW alignment beams (frame 1 and frame 2). It was found, that a rod shot or even full system shot can be approximated by using the fiber-launched, larger-focused Frame 1 CW-beam, while the Frame 2 beam with its near-perfect beam quality can provide a measurement of the ‘ideal’ focus distribution.

Figure 3-6 compares the foci of the LLE800 phase plate for both frames. As expected, the focus with the alignment beam of Frame 2 is smaller (by about 10%). We also observe a deeper modulation.

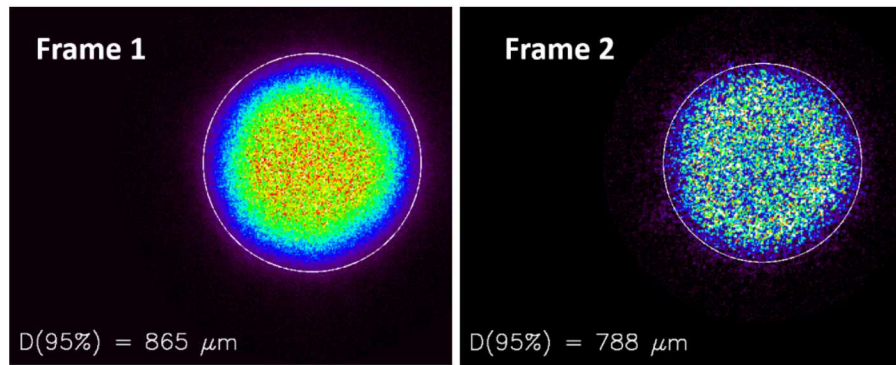


**Figure 3-6. Comparison of focus distributions for the LLE800 phase plate with the two alignment laser for Frame 1 and Frame 2 of Z-Beamlet.**

#### 3.3.1. Angular intensity variations

While subtle, one can see that the speckle distribution in Frame 2 is not entirely even over the focal area. Lineouts across the focus at varying angles show that the center intensity does not vary much, but the intensity near the edge of the focus can vary noticeably as seen in Fig. 3.7:

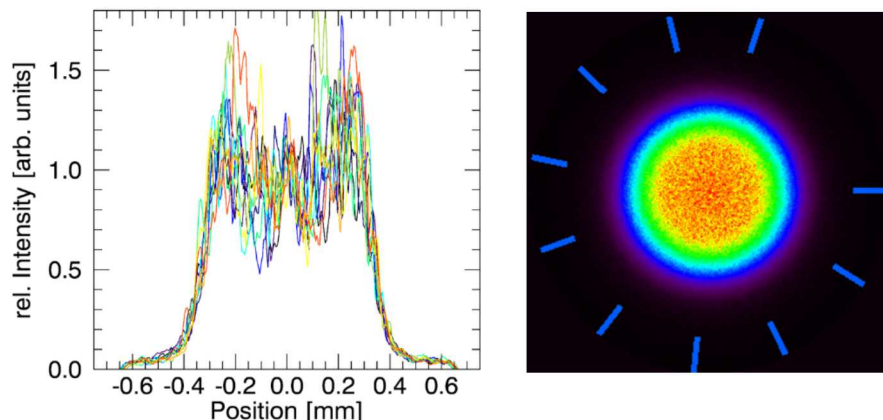


**Figure 3-7. Lineouts in  $32^\circ$  increments (actual directions indicated by blue lines on the right hand image) show noticeable intensity variations along the edge of the focus profile.**

### 3.4. Characteristics of the SNL750 Phase Plate

After promising experiments with loaner phase plates from the University of Rochester, Sandia decided to purchase similar optics. A more thorough characterization was performed for these phase plates. SNL750 is based on a 750  $\mu\text{m}$  D95 design for LLE's Omega-EP laser (more precisely 736  $\mu\text{m}$  with acceptance of a 15  $\mu\text{m}$  error). The 'precise' D95 value measured at Sandia was 775  $\mu\text{m}$ , while the encircled energy at for the calculated D95 diameter shrunk to 92.7%. Because of imperfections in the background subtractions of these measurements, those values can be considered close enough. Figure 3.8 shows images and encircled-energy plots for the "Frame 2" alignment beam and a pulsed Z-Beamlet measurement that mimics a full system shot's distribution.

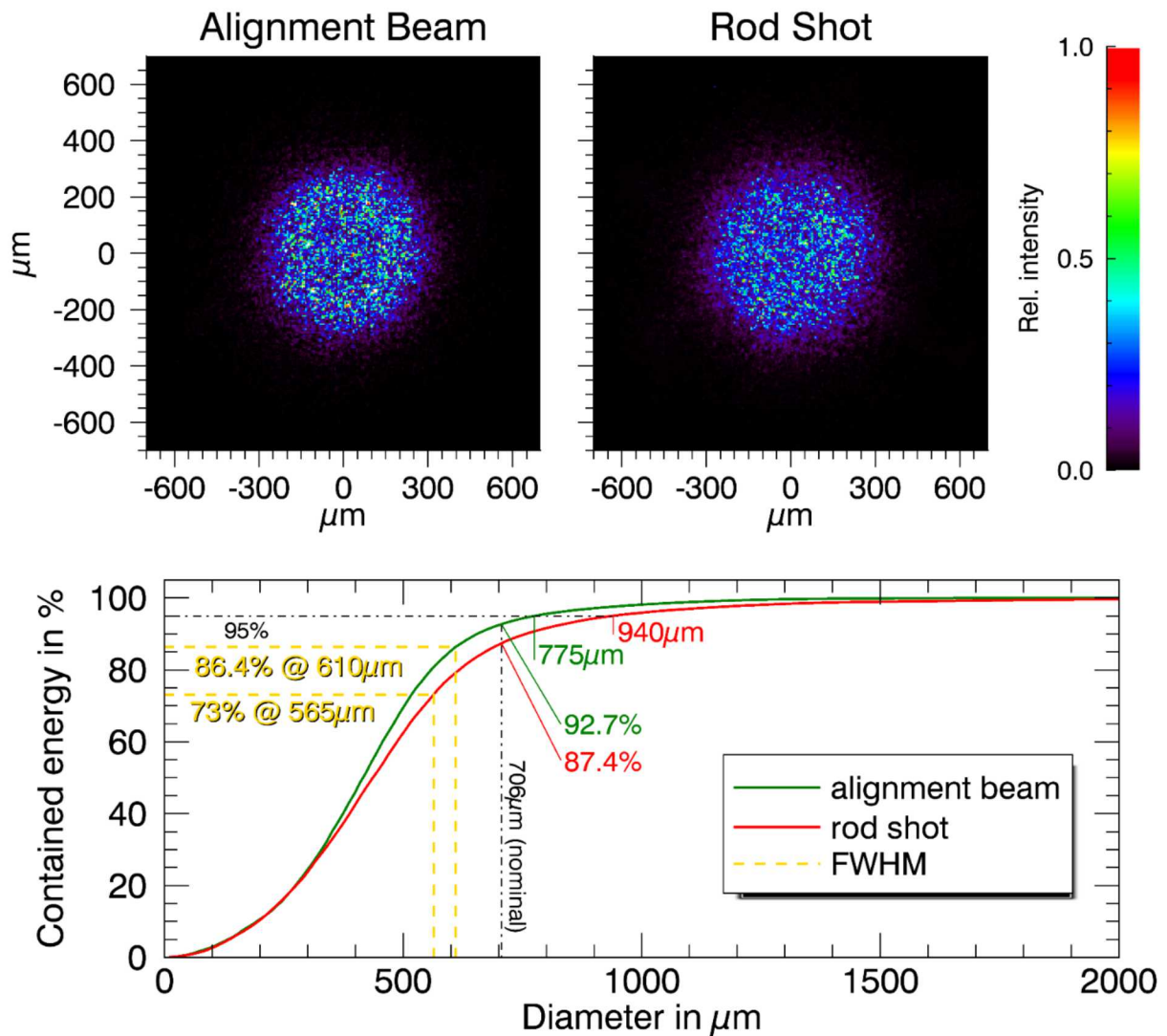
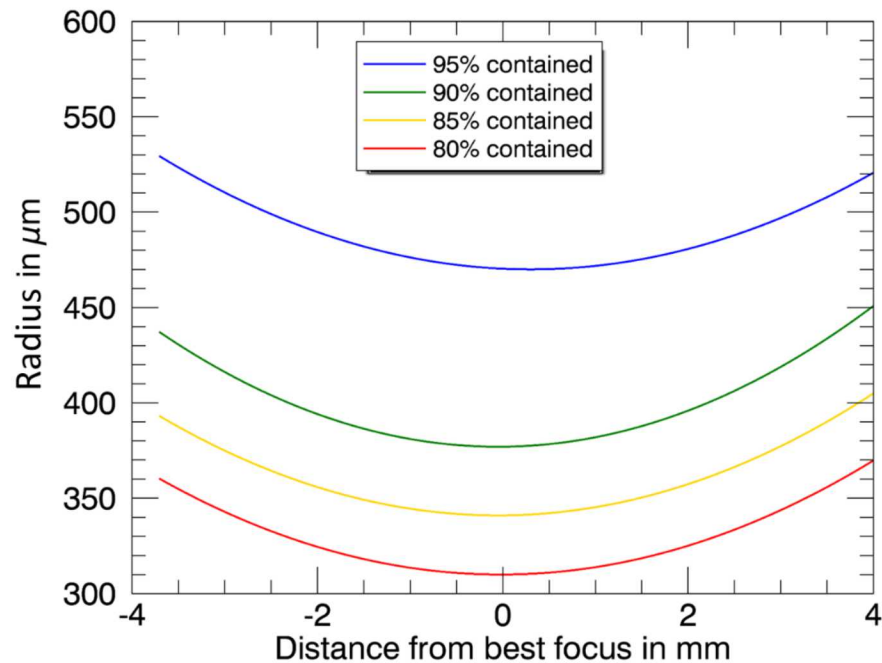


Figure 3.8. Characterization of the SNL750 phase plate.

The beam waist measurement for the SNL750 phase plate shows virtually no change of focus within  $\pm 0.5$  mm around the focal plane, as shown in Fig. 3.9:



**Figure 3.9. SNL750 beam waist.** Actual data points are not shown. Plots represent a Gaussian approximation of the measured data points.

### 3.5. Characteristics of the SNL1100 Phase Plate

After finding that LPI was much reduced for MagLIF experiments with a larger phase plate, the standard for conditioned focus experiments (as compared to not having a phase plate) quickly became the optic with a  $D95 = 1100 \mu\text{m}$  design. It has been used for all shots with 90 psi and 120 psi target fills. Figure 3.10 shows the synopsis of the characterization measurements.

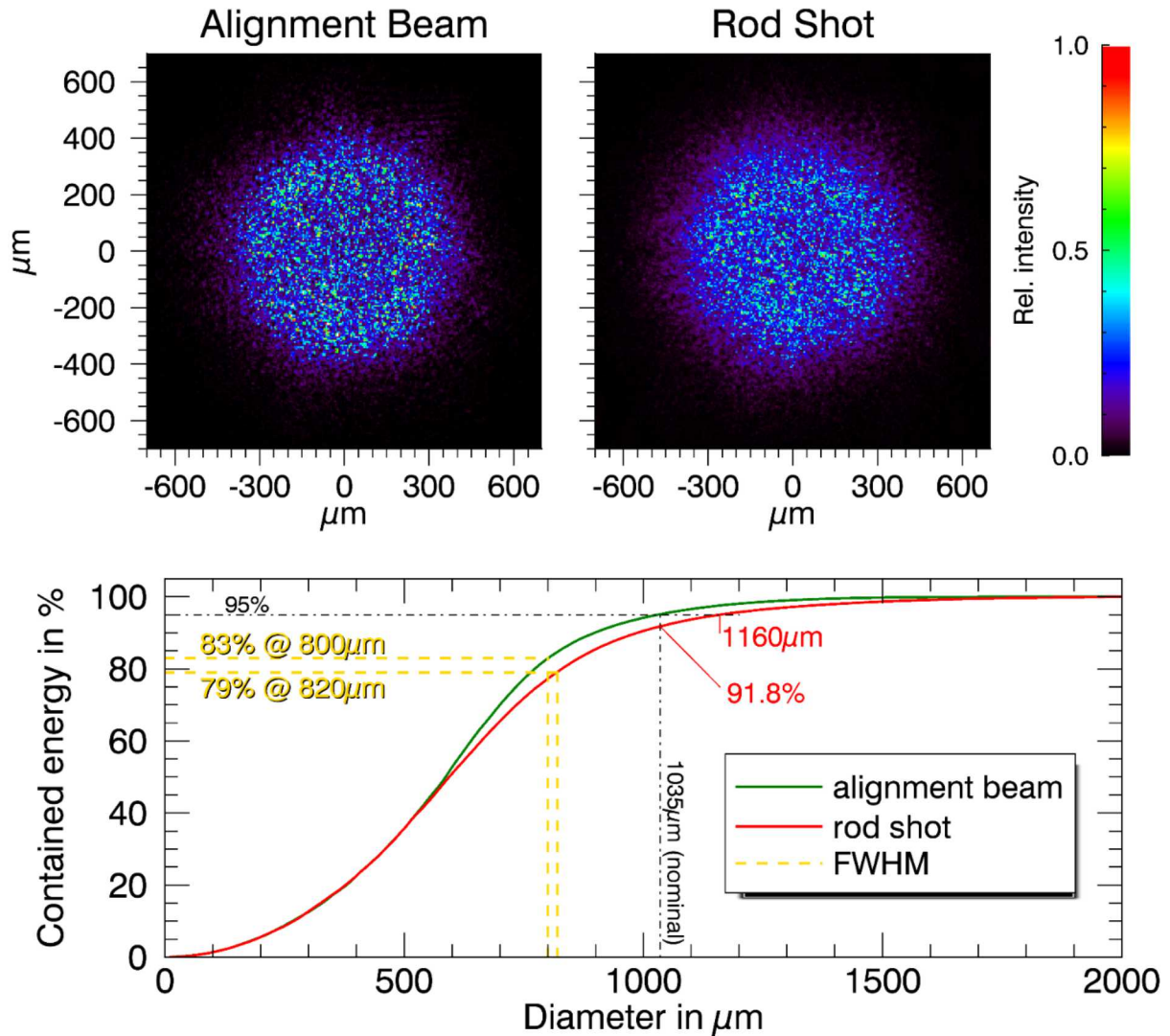


**Figure 3-10. Characterization of the SNL750 phase plate.**

As one might expect the beam waist is even less sensitive to a deviation from best focus as shown in Fig. 3.11. A mismatch of  $\pm 1 \text{ mm}$  is likely insignificant for experiments unless a softening of the edge leads to clipped energy on an aperture (see Fig. 3.1).

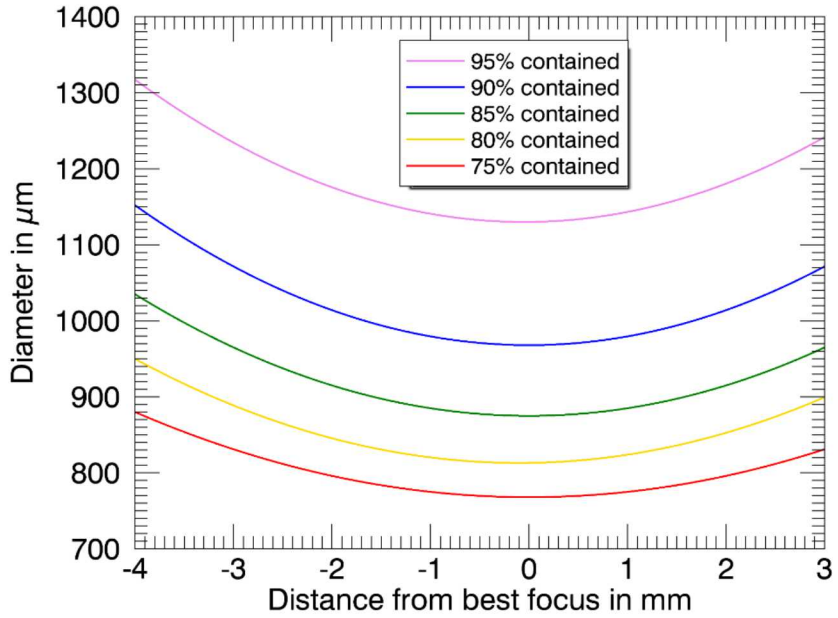


**Figure 3-11. SNL1100 beam waist. Actual data points are not shown. Plots represent a Gaussian approximation of the measured data points.**

### 3.5.1. Focus shape with phase plate reversal

We used the SNL1100 phase plate to investigate whether there is a penalty from accidentally inserting the phase plate ‘backwards’. There was no obvious problem with doing so as demonstrated in Fig. 3.12. Only under close scrutiny can a difference of 0.5% energy containment at a given radius be seen. This may very well be caused by uncertainties in the background correction for the data.

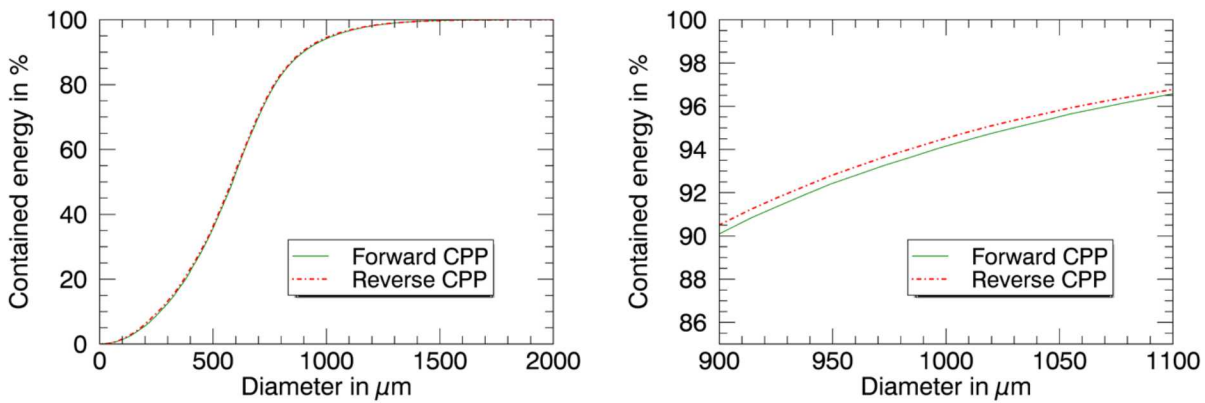


**Figure 3-12. Comparison of encircled energies for forward and reverse phase plate insertions.** The abbreviation ‘CPP’ stands for ‘continuous phase plate’ and is synonymous to ‘distributed phase plate (DPP)’, depending on the terminology of individual laser facilities.

### 3.6. Characteristics of the SNL1500 Phase Plate

Experiments for Magnetized Liner Inertial Fusion indicated that, when Z-Beamlet were to deliver pre-heat energy in excess of 3 kJ to the target, a larger spot diameter will be needed to avoid exceeding the depth of the target and to minimize losses caused by laser-plasma instabilities at higher densities. A larger design was created, for the first time by personnel at Sandia (SNL ORG-01682; Jens Schwarz), with a nominal diameter of 1.58 mm for an encircled energy of 95%, using a 3.2m focusing lens (such as the focusing lens in Z and in the PECOS target chamber).

The design was imprinted by Zygo Corporation on an SNL-provided substrate and later characterized in the PECOS target chamber as shown in Fig. 3.13. The measurements confirmed that the final product resulted in a focus shape that resembles the numerical design very closely, probably within the measurement error (while hard to assess, we assume that the measurement precision is around 10-20  $\mu\text{m}$ ). The D95 value seems insensitive on the beam quality (rod vs. CW).

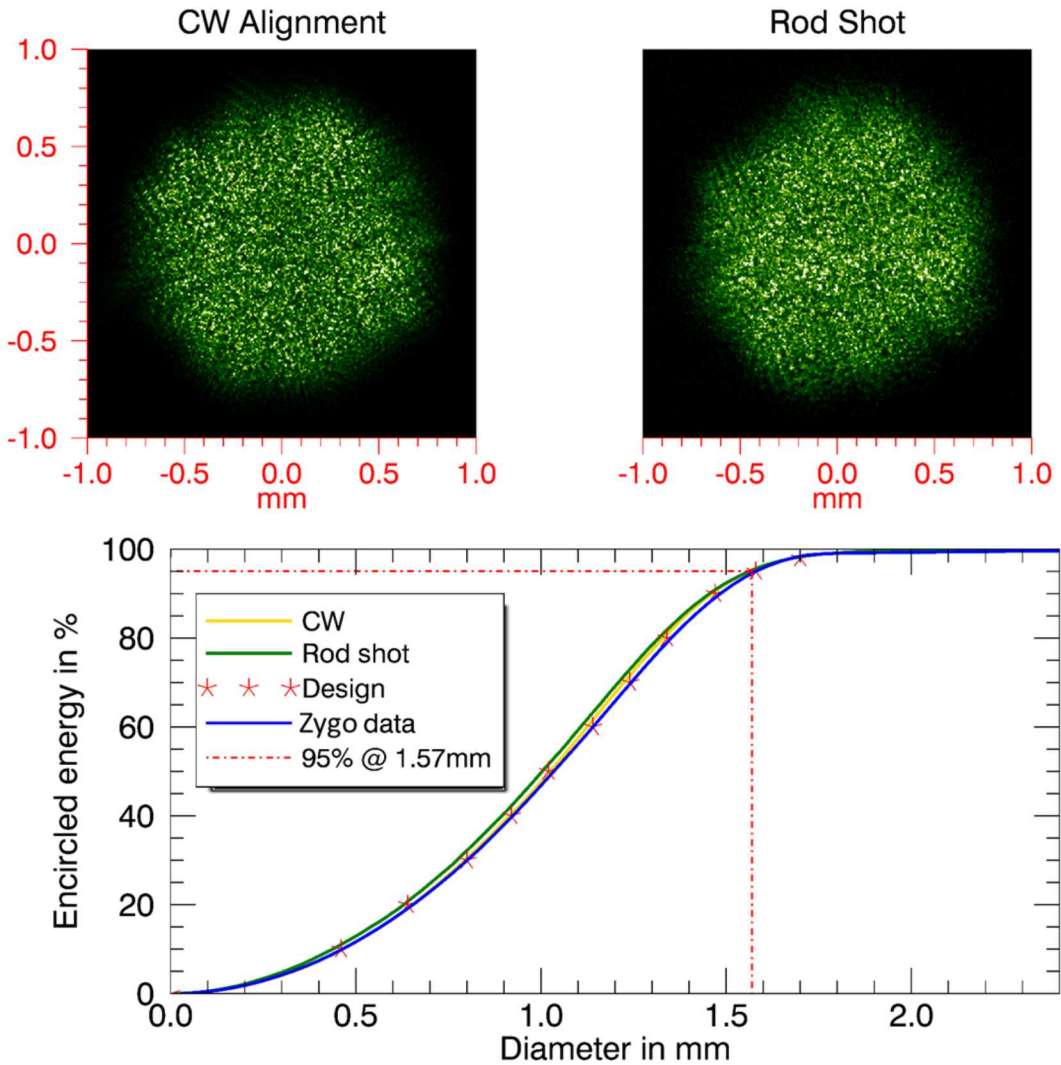
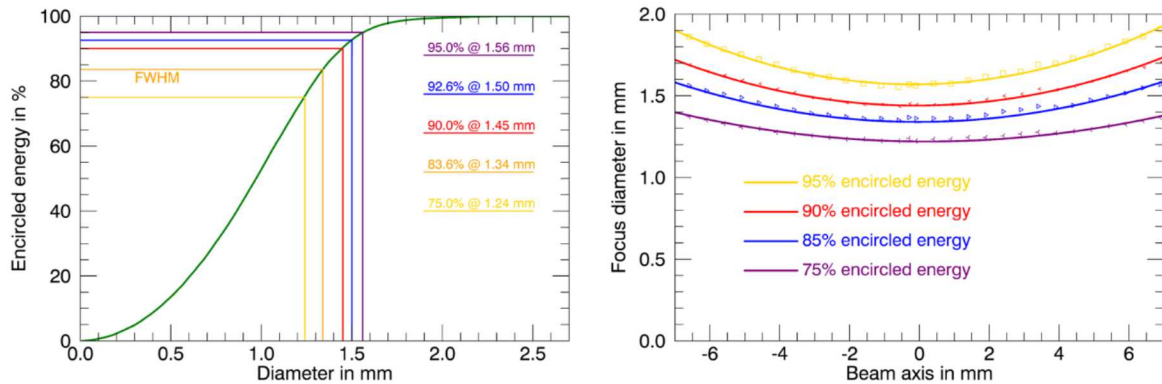


Figure 3-13. Characterization of the SNL750 phase plate.

Figure 3.13 shows that the high quality metrology system of Zygo measured a focus distribution that is reproducing the design almost perfectly. Real-life data with the Z-Beamlet laser have slight deviations, but are still encouragingly close. Figure 3.14 shows the beam-waist measurements and a more detailed characterization of the encircled energy at best focus.



**Figure 3-14. Specific diameter/energy combinations (left) and beam waist data (right) for the SNL1500 phase plate. The waist is practically flat over an depth exceeding  $\pm 1$  mm**

A complete synopsis of encircled energy data is given by table 3.2, which shows the excellent agreement between Z-Beamlet focus data and design, as well as the insensitivity of the phase plate to the type of beam used for the measurement. The latter is likely a benefit arising from the overall rather large focus with slightly soft edges.

**Table 3-1. List of Encircled energy diameters for the SNL1500 phase plate (all diameter measurements in mm).**

Encircled energy [%]	Design Diameter	CW Diameter	Rod Shot Diameter
10	0.46	0.47	0.44
20	0.64	0.65	0.63
30	0.80	0.79	0.77
40	0.92	0.92	0.89
50	1.02	1.03	1.00
60	1.14	1.12	1.11
70	1.24	1.22	1.21
80	1.34	1.33	1.32
90	1.47	1.46	1.46
95	1.58	1.57	1.56
98	1.70	1.68	1.68

## DISTRIBUTION

### Email—Internal

Name	Org.	Sandia Email Address
Sinars, Daniel	01600	<a href="mailto:dbsinar@sandia.gov">dbsinar@sandia.gov</a>
Peterson, Kyle	01655	<a href="mailto:kpeters@sandia.gov">kpeters@sandia.gov</a>
Bliss, David	01659	<a href="mailto:debliss@sandia.gov">debliss@sandia.gov</a>
Bourdon, Chris	01670	<a href="mailto:cjbourd@sandia.gov">cjbourd@sandia.gov</a>
Fein, Jeffrey	01676	<a href="mailto:jrfein@sandia.gov">jrfein@sandia.gov</a>
Rochau, Gregory	01680	<a href="mailto:garocha@sandia.gov">garocha@sandia.gov</a>
Jones, Michael	01681	<a href="mailto:micjone@sandia.gov">micjone@sandia.gov</a>
Colombo, Anthony	01682	<a href="mailto:apcolom@sandia.gov">apcolom@sandia.gov</a>
Edens, Aaron	01682	<a href="mailto:adedens@sandia.gov">adedens@sandia.gov</a>
Field, Ella	01682	<a href="mailto:efield@sandia.gov">efield@sandia.gov</a>
Galloway, Benjamin	01682	<a href="mailto:brgallo@sandia.gov">brgallo@sandia.gov</a>
Geissel, Matthias	01682	<a href="mailto:mgeisse@sandia.gov">mgeisse@sandia.gov</a>
Kimmel, Mark	01682	<a href="mailto:mwkimme@sandia.gov">mwkimme@sandia.gov</a>
Kletecka, Damon	01682	<a href="mailto:dkletec@sandia.gov">dkletec@sandia.gov</a>
Porter, John	01682	<a href="mailto:jlporte@sandia.gov">jlporte@sandia.gov</a>
Rambo, Patrick	01682	<a href="mailto:prambo@sandia.gov">prambo@sandia.gov</a>
Schollmeier, Marius	01682	<a href="mailto:mscholl@sandia.gov">mscholl@sandia.gov</a>
Schwarz, Jens	01682	<a href="mailto:jschwar@sandia.gov">jschwar@sandia.gov</a>
Shores, Jonathon	01682	<a href="mailto:jeshore@sandia.gov">jeshore@sandia.gov</a>
Smith, Ian	01682	<a href="mailto:icsmith@sandia.gov">icsmith@sandia.gov</a>
Speas, Robert	01682	<a href="mailto:rjspeas@sandia.gov">rjspeas@sandia.gov</a>
Speas, Shane	01682	<a href="mailto:csspeas@sandia.gov">csspeas@sandia.gov</a>
Ampleford, David	01683	<a href="mailto:damplef@sandia.gov">damplef@sandia.gov</a>
Dunham, Gregory	01683	<a href="mailto:gsdunha@sandia.gov">gsdunha@sandia.gov</a>
Gomez, Matthew	01683	<a href="mailto:mrgomez@sandia.gov">mrgomez@sandia.gov</a>
Harding, Eric	01683	<a href="mailto:ehardin@sandia.gov">ehardin@sandia.gov</a>
Harvey-Thompson, Adam	01683	<a href="mailto:ajharve@sandia.gov">ajharve@sandia.gov</a>
Awe, Thomas	01688	<a href="mailto:tjawe@sandia.gov">tjawe@sandia.gov</a>
Jones, Brent	01688	<a href="mailto:bmjones@sandia.gov">bmjones@sandia.gov</a>
Knapp, Patrick	01688	<a href="mailto:pfknapp@sandia.gov">pfknapp@sandia.gov</a>
Kellogg, Jeffrey	01691	<a href="mailto:jwkello@sandia.gov">jwkello@sandia.gov</a>
Robertson, Grafton	01692	<a href="mailto:grober@sandia.gov">grober@sandia.gov</a>
Technical Library	01177	<a href="mailto:libref@sandia.gov">libref@sandia.gov</a>



This page left blank

This page left blank



**Sandia  
National  
Laboratories**

Sandia National Laboratories is a multimission laboratory managed and operated by National Technology & Engineering Solutions of Sandia LLC, a wholly owned subsidiary of Honeywell International Inc. for the U.S. Department of Energy's National Nuclear Security Administration under contract DE-NA0003525.